118.

W. VLA OBSERVATIONS OF THE CORONAL PLASMA

Kenneth R. Lang, Tufts University

IAU SYMPOSIUM No. 142

BASIC PLASMA PROCESSES ON THE SUN

Bangalore, India

December 1-5, 1989

VLA OBSERVATIONS OF THE CORONAL PLASMA

KENNETH R. LANG
Dept. of Physics and Astronomy
Tufts University
Medford, MA 02155
U.S.A.

ABSTRACT. VLA observations at 20-cm wavelength specify the brightness temperature and magnetic structure of plasma constrained within coronal loops in solar active regions. Comparisons with simultaneous SMM observations at soft X-ray wavelengths lead to measurements of physical parameters like electron density, electron temperature and magnetic field strength. Such comparisons also indicate coronal loops can be detected at either radio or X-ray wavelengths while remaining invisible in the other spectral domain, and that the dominant radiation mechanisms can be thermal bremsstrahlung or thermal gyroresonance radiation. VLA observations at the longer 90-cm wavelength reveal the thermal emission of a hot transition sheath enveloping a cooler, underlying Hα filament seen in absorption. The 20-cm VLA observations indicate that the precursor, impulsive and post-flare components of solar flares originate in spatially separated and resolved sources. The 90-cm VLA data indicate that time-correlated radio bursts can occur in active regions on opposite sides of the solar equator. These regions are apparently linked by large-scale, trans-equatorial magnetic loops at least 2.6×10^5 km (or 6') long; these loops act as magnetic conduits for relativistic electrons moving at one-third the velocity of light.

I. INTRODUCTION.

This paper provides a brief overview of recent discoveries by the Tufts University group using the Very Large Array (VLA) to study the coronal plasma under the support of the AFOSR and NASA (Section 6). More detailed accounts can be found in the references given in this introduction and in Section 7. Ground-based VLA observations at 20-cm wavelength can detect the hot coronal plasma previously detected by space-bourne X-ray telescopes; detailed comparisons of simultaneous data (SMM and VLA) indicate that physical parameters can be obtained (Section 2), but that some coronal loops are invisible in either spectral domain. (Lang, Willson, Smith and Strong 1987a,b). At the longer 91.6-cm wavelength, the VLA detects more extensive emission interpreted

as a hot 10^5 K interface between cool, dense Hα filaments and the hotter, enveloping rarefied corona (Section 3, Lang and Willson, 1989a). The unparalleled spatial resolution of the VLA at 20-cm wavelength has shown that the precursor, impulsive and post-flare components of solar bursts originate in nearby, but separate, coronal loops or systems of loops (Section 4, Willson, Lang and Liggett, 1990; Willson, Klein, Kerdraon, Lang and Trottet, 1990). Flaring emission detected at 90-cm wavelength reveals otherwize-invisible, trans-equatorial loops that act as magnetic conduits for relativistic electrons that trigger flares on opposite sides of the solar equator (Section 5, Lang and Willson, 1989b).

2. QUIESCENT 20 CM AND X-RAY EMISSION FROM CORONAL LOOPS

The development of aperture synthesis telescopes like the Very Large Array (VLA) has permitted ground-based observations of coronal loops at 20-cm wavelength; the quiescent, or non-flaring, loop emission has brightness temperatures, T_B, comparable to the million-degree coronal electron temperature. A comparison with simultaneous soft X-ray images of comparable angular resolution and field of view (Fig.1) indicates that X-ray coronal loops can be completely imaged at 20 cm.

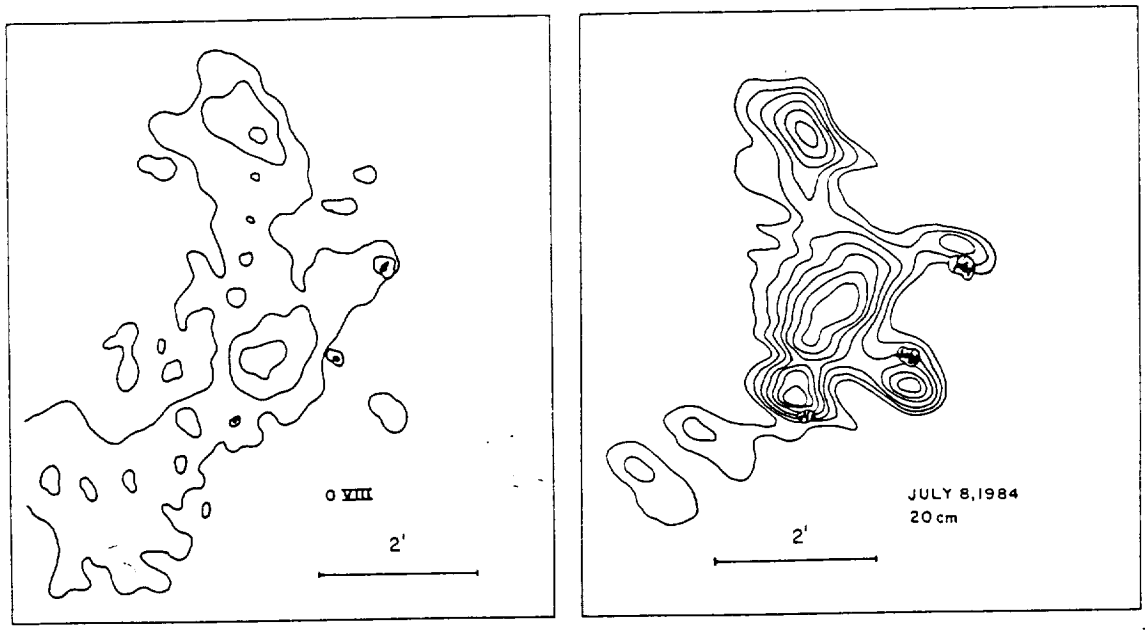

Figure 1. A comparison of soft X-ray (SMM FCS - left) and 20-cm (VLA-right) images of an active region. Here the sunspots are denoted by small black dots with a circle around them, and the identical angular scale for the two images can be inferred from the 120" spacing between the fiducial marks on the axes. The soft X-ray data were taken in the O VIII line (18.0 A); they show two regions of hot, million-degree plasma that are also detected at 20 cm. The radio image also shows hot regions near sunspots that are not detected with soft X-rays. The contours of the 20-cm map mark levels of equal brightness temperature corresponding to 0.4, 0.5, 0.6, ... 1.0 times the maximum brightness temperature of 1.4×10^6 K. (Adapted from Lang et al. (1987a)).

Soft X-ray spectral lines have been used to determine the electron temperature, T_e, and electron density, N_e, of the X-ray emitting plasma that spatially coincides with the 20-cm radiation; for the data shown in Fig. 1, average values of $T_e = 3.0 \pm 0.1 \times 10^6$ K and $N_e = 2.4 \pm 0.4 \times 10^9$ cm^{-3} were obtained. The quiescent X-ray radiation is attributed to thermal bremsstrahlung. The 20-cm emission is optically thin with optical depths $\tau = T_e/T_B = 0.3$. The thermal bremsstrahlung of the X-ray emitting plasma ought to be optically thin at 20 cm, but its thermal gyroresonance radiation should be optically thick at this wavelength. The low T_B is then explained if a higher, cooler plasma covers the hotter X-ray emitting plasma. Thermal gyroresonance radiation must account for the intense 20-cm radiation near and above sunspots where no X-ray radiation is detected (also see Fig. 1).

3. QUIESCENT 90 CM EMISSION FROM FILAMENTS.

Although 20-cm VLA observations of the quiet Sun reveal the ubiguitous coronal loops anchored within solar active regions, the VLA results at the longer 91.6-cm wavelength reveal quiescent emission from more extensive structures (angular sizes $\theta = 3'$) that are not associated with active regions (Fig. 2 right and left). The 91.6-cm features are similar in shape, position, elongation and orientation to dark Hα filaments; but the radio structures are wider and longer, and they are detected in emission rather than absorption. This 91.6-cm emission has been interpreted as the thermal bremsstrahlung of a hot (10^5 K), thin (10^4 km) transition sheath that envelopes the cooler Hα filaments and acts as an interface with the hotter surrounding corona; this sheath is seen in emission because of the relatively low optical depth of the low-density corona.

Comparisons of the observed brightness temperatures, as corrected for the contribution of the corona, with theoretical models, and with other observations at shorter radio wavelengths, indicate that a power-law gradient in pressure provides a better fit than a constant pressure model (Lang and Willson, 1989a). Variable physical parameters of the transition sheath can explain controversial reports of the detection of, or the failure to detect, the meter-wavelength counterpart of Hα filaments. If the sheath were substantially thinner, then the optical depth would not be large enough for detection of its 91.6-cm bremsstrahlung; and if the electron density of the sheath was much higher than $N_e = 10^9$ cm^{-3}, then its plasma frequency would exceed our observing frequency and the sheath radiation could not propagate out to be observed.

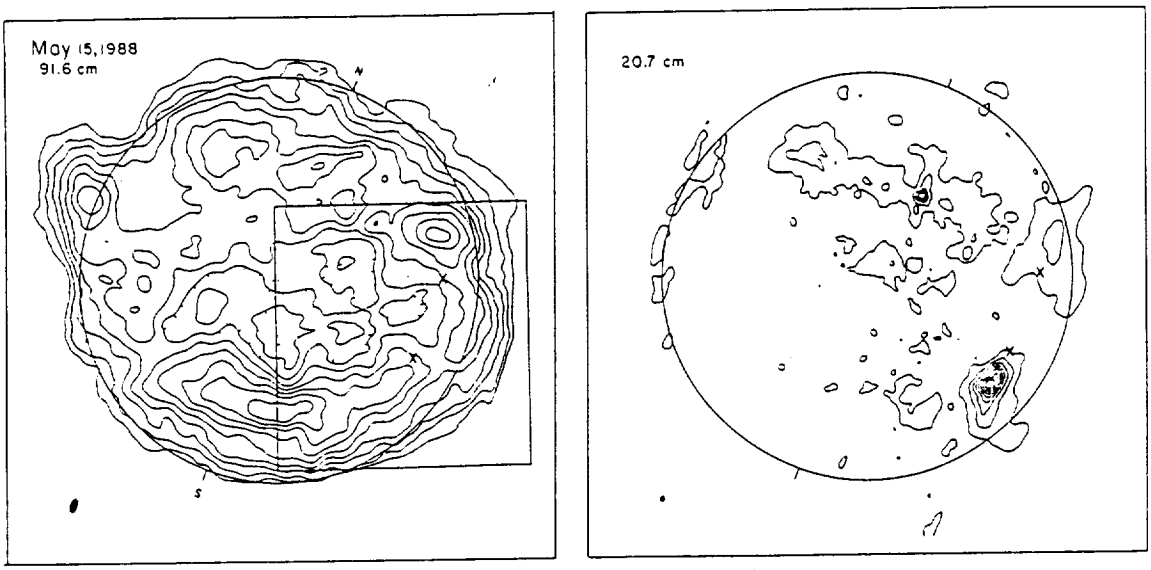

Figure 2. Three-hour VLA synthesis maps of the quiescent, or non-flaring, intensity from the visible solar disk at 91.6 cm (left) and 20.7 cm (right). The circle denotes the visible solar limb; the tick marks denote solar north and south; and the synthesized beamwidths are denoted by the dark spots in the lower left-hand corners. The 20.7-cm contours delineate active-region coronal loops with a peak brightness temperature of $T_B = 2.5 \times 10^6$ K, while the 91.6-cm contours show more elongated structures that are not associated with active regions and have a peak $T_B = 7.8 \times 10^5$ K. The dominant 91.6-cm emission in the southern hemisphere coincides with a dark, underlying Hα filament; the emission (91.6-cm) and absorption (Hα) features have a similar shape, position, elongation and orientation; but the 91.6-cm emission is wider and longer, suggesting a warm transition sheath that acts as an interface between the cool, dense Hα filament and the hot, rarefied enveloping corona. (Adapted from Lang and Willson (1989a)).

4. RESOLVING FLARE COMPONENTS

The classical time profile for the microwave or radio emission of solar flares, or eruptions, consists of a low-level precursor, and a rapid powerful impulsive component, followed by a more gradual post-burst, or decay, phase (see Fig. 3). The VLA has now been used to map these flaring components at 3-second time intervals, showing that they originate in spatially separated sources (Fig 4 and 5).

These results suggest that solar flares are triggered by interacting coronal loops; emerging coronal loops may interact with adjacent ones, leading to the explosive release of magnetic energy stored within them. The system of coronal loops then relaxes to a spatially-different configuration during the decay phase. Comparisons with various theoretical models indicate that a multithermal model with magnetic field strengths of H = 75 to 120 G can explain the impulsive component. Thermal gyroresonance emission from coronal loops with H < 270 G can explain the precursor source; both the 20.7-cm and hard

X-ray emission during the impulsive phase can be attrubuted to non-thermal electrons in the coronal and chromospheric portions of magnetic loops (Willson, Lang and Liggett, 1990; Willson et al., 1990).

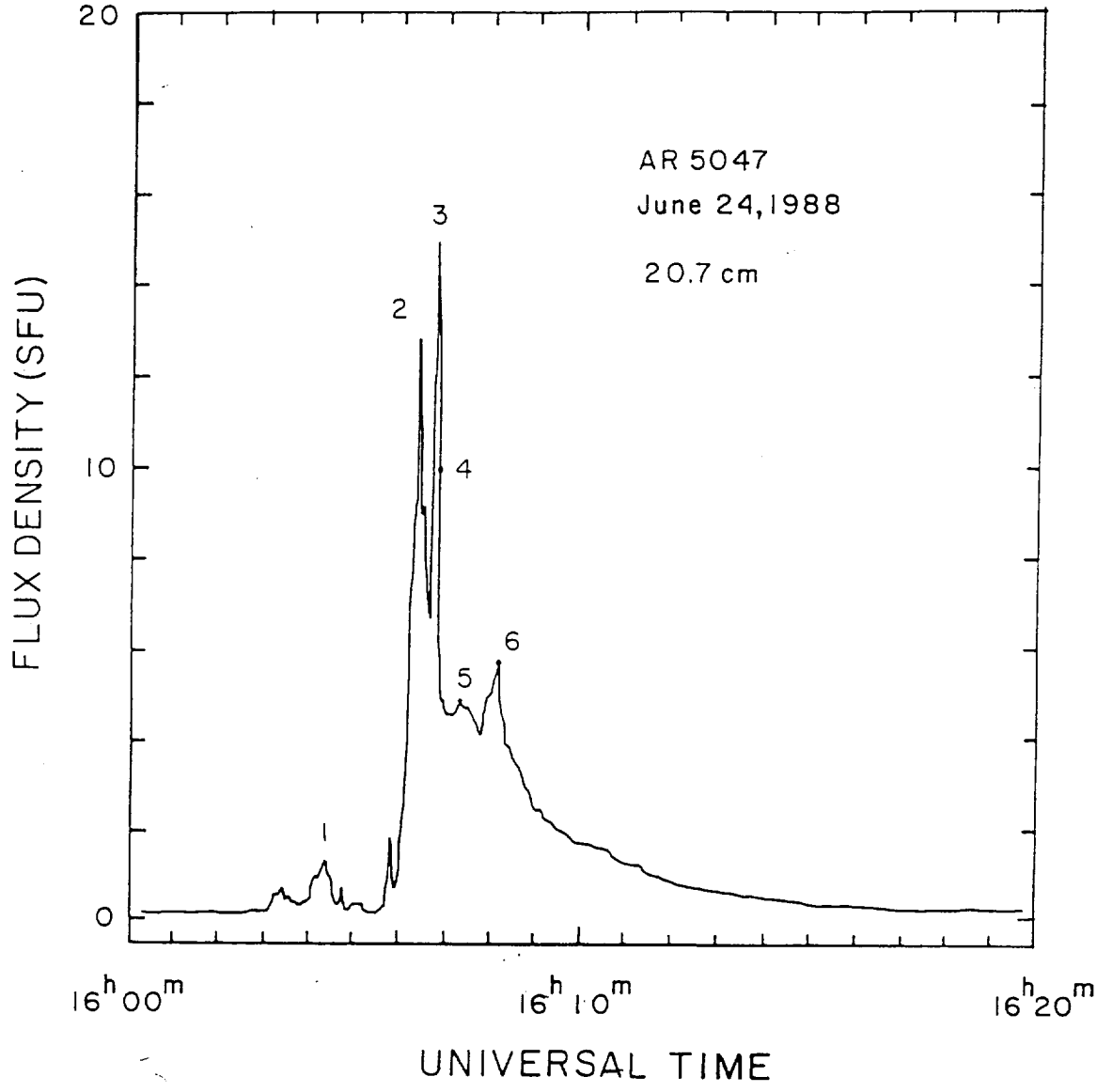

Figure 3. The time profile of a 20.7-cm burst showing the preburst (1), impulsive (2,3), and post-burst (4,5,6) phases. The VLA snapshot maps given in Fig. 4 indicate that these three phases originate from spatially separated, resolved components. (Adapted from Willson, Lang and Liggett (1990)).

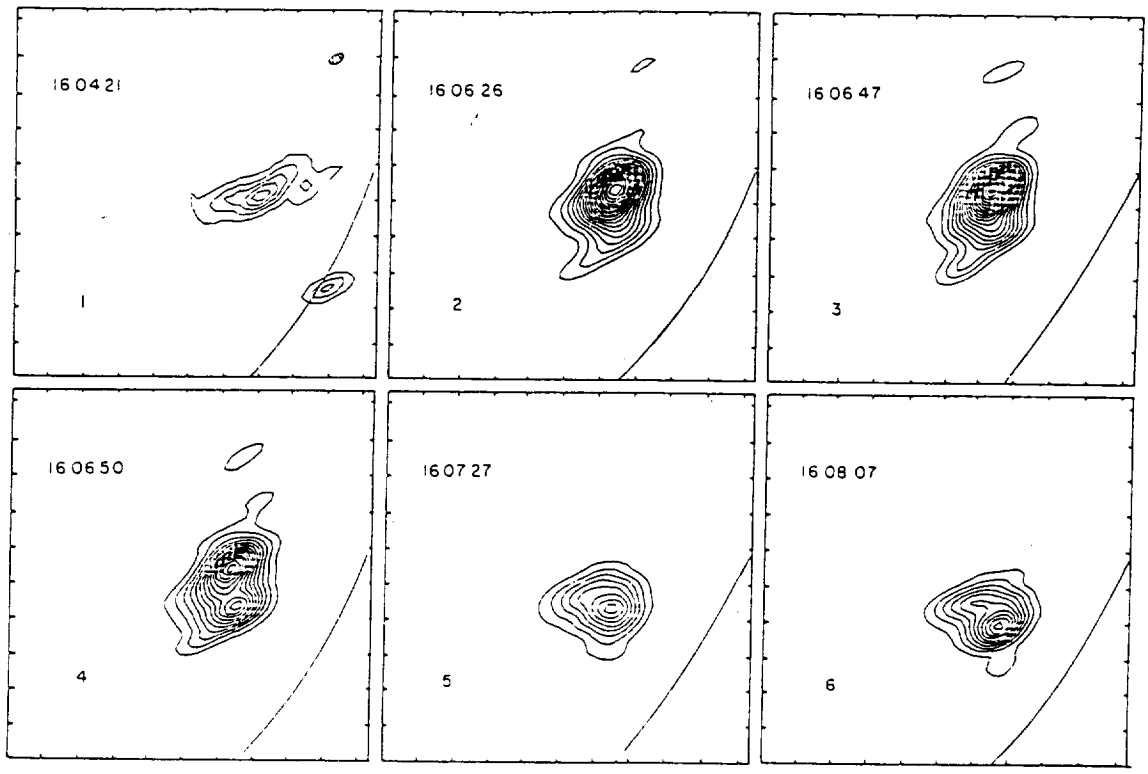

Figure 4. VLA snapshot maps of the total intensity, I, at 20.7-cm wavelength during 3.3-second intervals at the times denoted by 1 to 6 in Fig. 3. The precursor (1) is spatially separated from the subsequent impulsive bursts (2 and 3). The post-burst, or decay, phase (5,6) originates in another spatially separate source that first becomes detectable during the end (4) of the second impulsive burst (3). All three components are resolved with a synthesized beamwidth of 12" x 30"; the angular scale can be inferred from the 60" spacing between the fiducial marks on the axes. The contour intervals are in units of equal brightness temperature, T_B, with an outermost contour and contour interval of $T_B = 4.4 \times 10^5$ K for 1, and $T_B = 5.5 \times 10^6$ K for the others five images. The maximum value is $T_{Bmax} = 4.4 \times 10^6$, 1.0×10^8, 1.3×10^8, 7.7×10^7, 4.4×10^7 and 5.5×10^7 K for 1,2,3,4,5 and 6 respectively. (Adapted from Willson, Lang and Liggett (1990)).

5. TRIGGERING FLARES ACROSS TRANS-EQUATORIAL LOOPS

Time-correlated radio bursts have been observed in active regions on opposite sides of the solar equator (Figs. 6 and 7). These regions are apparently linked by large-scale, trans-equatorial magnetic loops that are at least 2.6×10^5 km (or 6') long. Energetic electrons accelerated during a radio burst in one active region probably move along this magnetic conduit at velocities of about one-third the velocity of light, thereby triggering radio bursts in the other active region.

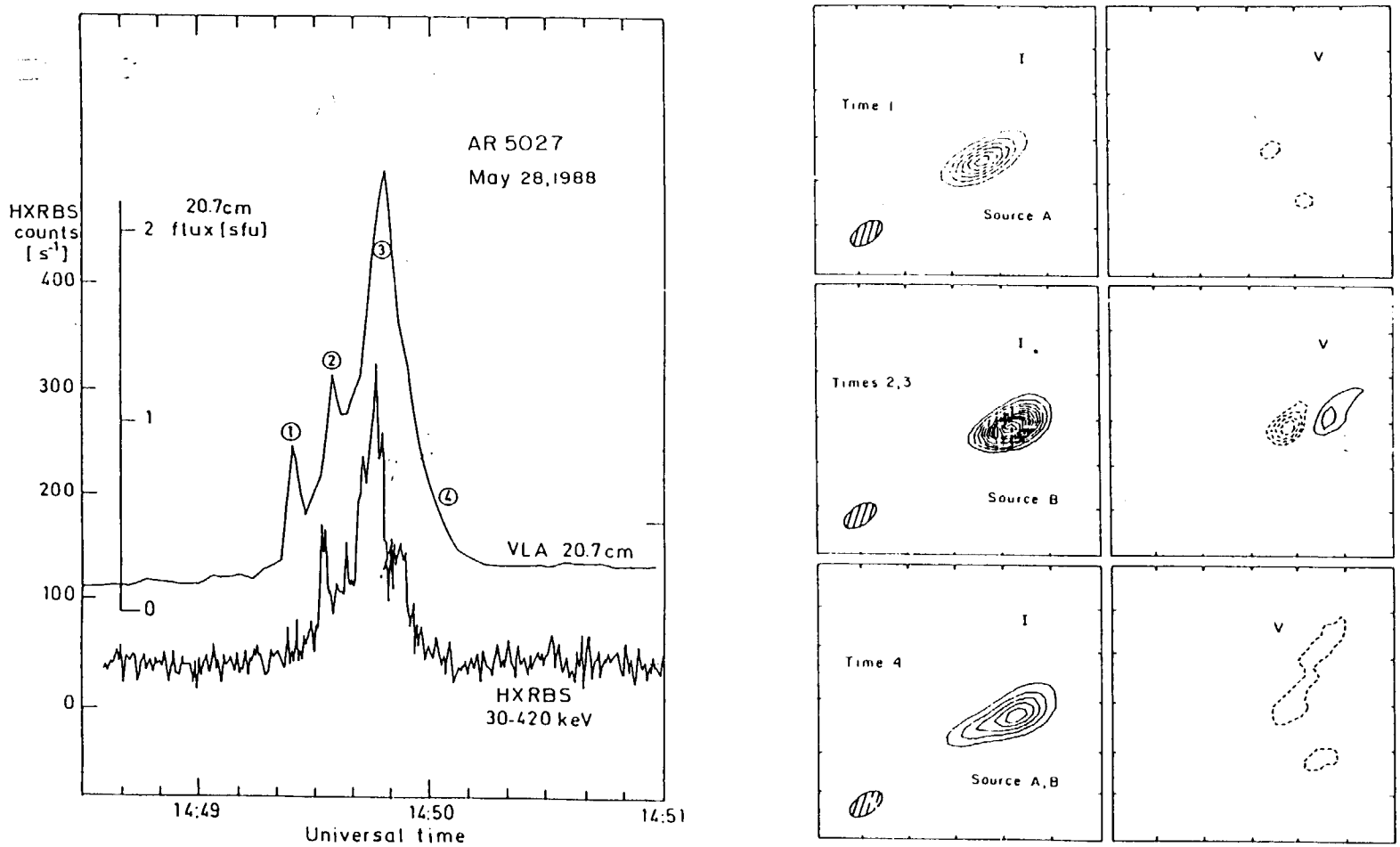

Figure 5. Time profiles (left) of the emission at 20.7-cm (VLA) and hard X-rays (SMM - HXRBS); and three-second VLA snapshot maps (right) of the total intensity, I, and circular polarization, V, at 20.7 cm for the times denoted 1 to 4 in the time profile. Although the first 20.7 cm peak (designated 1) is not detected at hard X-rays, the rest of the burst profile (2,3 and 4) in the two spectral domains is very similar. The snapshot maps show spatially separated resolved sources.

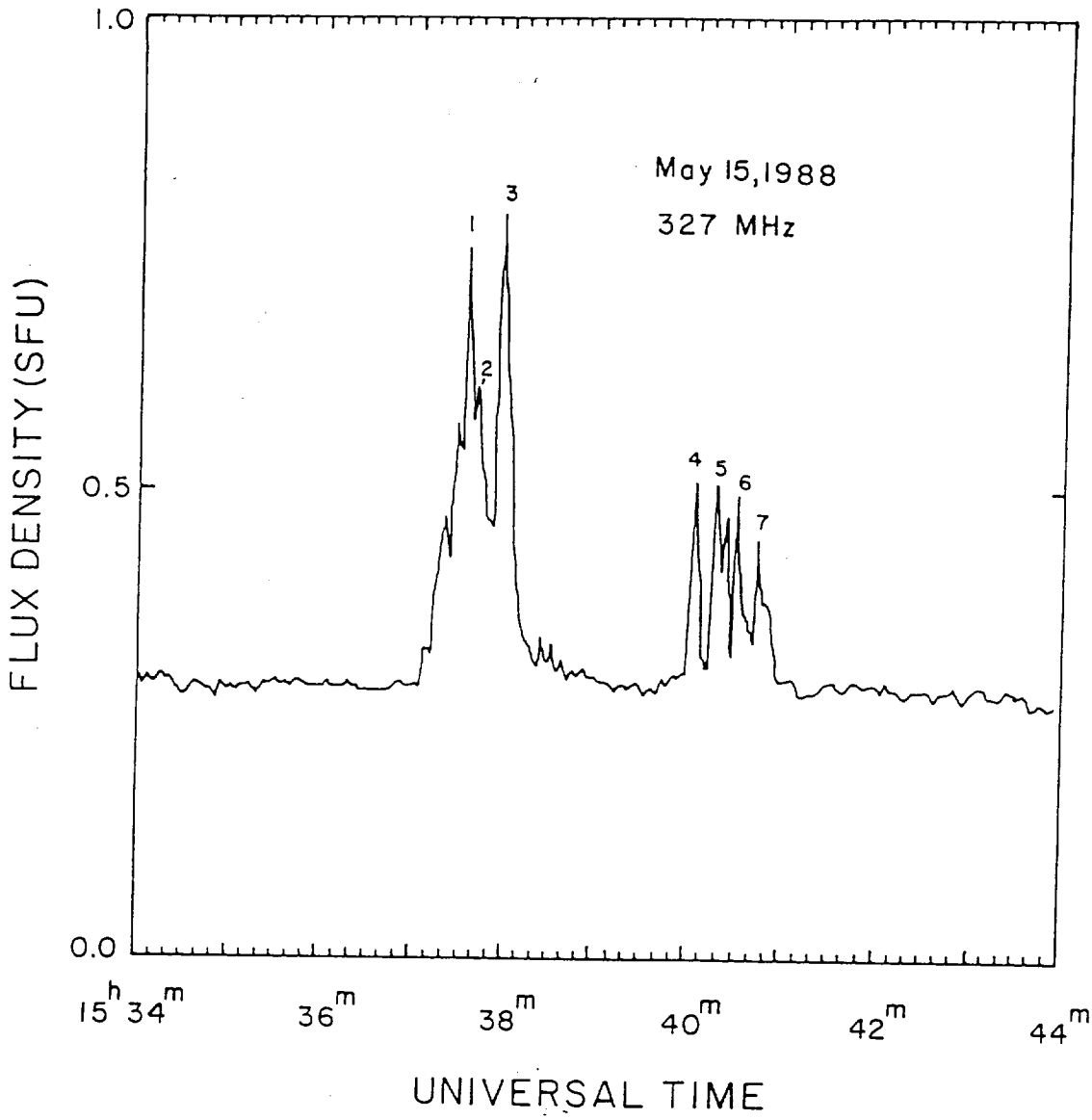

Figure 6. Time profile of the 91.6-cm (327 MHz) emission detected with one of the short VLA baselines (fringe spacing of about 5'). The VLA snapshot maps at times 1,2,3,4 and 5 are shown in Fig. 7. (Adapted from Lang and Willson (1989b)).

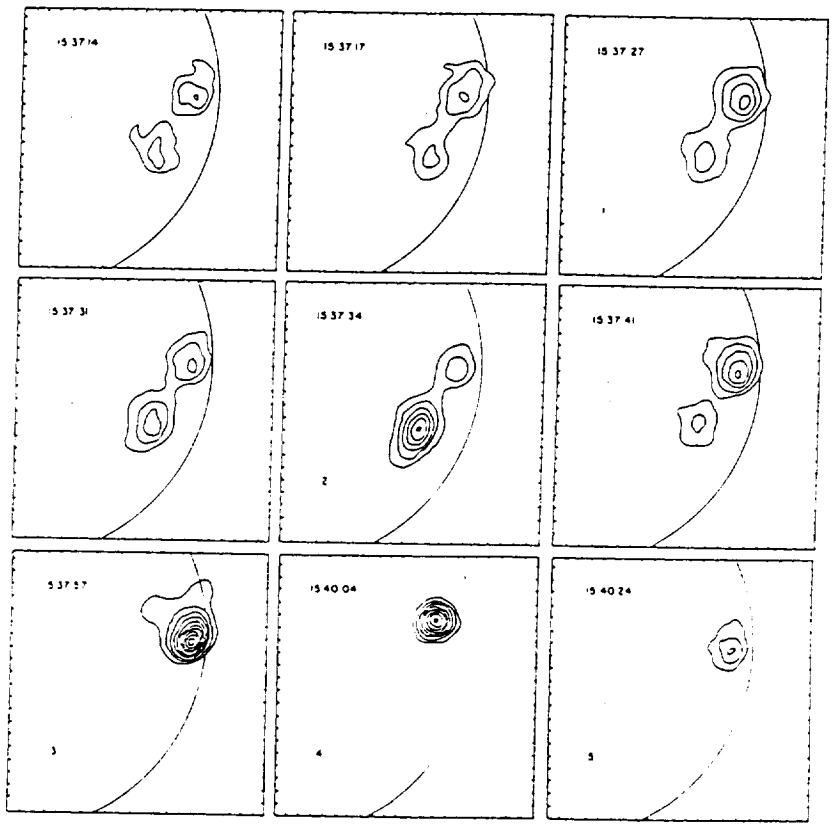

Figure 7. Three-second VLA snapshot maps at 91.6 cm for different times during the burst shown in Fig. 6. The emission comes from opposite sides of the solar equator in two regions separated by about 6', or 2.6 x 10^5 km; here the angular scale can be inferred from the 1' spacing between the fiducial marks on the axes. The contours mark intervals of equal brightness temperature, T_B, with an outermost contour and contour interval of 1 x 10^6 K. (Adapted from Lang and Willson (1989b)).

6. ACKNOWLEDGEMENTS.

Radio astronomical studies of the Sun at Tufts University are supported under grant AFOSR-89-0147 with the Air Force Office of Scientific Research. Related solar observations are supported by NASA grant NAG 5-501. The Very Large Array is operated by Associated Universities, Inc., under contract with the N.S.F.

7. REFERENCES.

Lang, K.R. and Willson, R.F. (1989a) 'Radio emission from quiescent solar filaments at 91.6 centimeter wavelength', Astrophysical Journal (Letters) 344, L73-L75.

Lang, K.R. and Willson, R.F. (1989b) 'Time-correlated bursts from widely separated solar active regions at 91.6 centimeter wavelength', Astrophysical Journal (Letters) 344, L77-L80.

Lang, K.R., Willson, R.F., Smith, K.L., and Strong, K.T. (1987a) 'Simultaneous SMM flat crystal spectrometer and Very Large Array Observations of solar active regions', Astrophysical Journal 322, 1035-1043.

Lang, K.R., Willson, R.F., Smith, K.L., and Strong, K.T. (1987b) 'Solar active region physical parameters inferred from a thermal cyclotron line and soft X-ray spectral lines', Astrophysical Journal 322, 1044-1051.

Willson, R.F., Klein, K.-L., Kerdraon, A., Lang, K.R., and Trottett, G. (1990) 'Multiple-wavelength analysis of energy release during a solar flare: thermal and non-thermal electron populations. Astrophysical Journal-submitted.

Willson, R.F., Lang, K.R., and Liggett, M. (1990) 'Impulsive microwave burst and solar noise storm emission resolved with the VLA', Astrophysical Journal, February 20, 1990.